# Relativistic Auger and x-ray emission rates of the $1s2s2p$ configuration of Li-like ions

Mau Hsiung Chen and Bernd Crasemann
*Department of Physics, University of Oregon, Eugene, Oregon 97403*

Hans Mark*
*Department of the Air Force, Washington, D.C. 20330*
(Received 9 February 1981)

Multiplet Auger and x-ray emission rates for the $1s2s2p$ configuration of Li-like ions ($13 \leq Z \leq 92$) have been calculated relativistically in the intermediate-coupling scheme, using Dirac-Hartree-Slater wave functions and the Møller two-electron operator. The effects of relativity on the Auger rates of the $^4P_{1/2}$ and $^4P_{3/2}$ states are found to be as large as two orders of magnitude. Relativity also very substantially affects the multiplet fluorescence yields of the $^4P_{1/2}$, $^4P_{3/2}$, and $^2P^{(+)}_{3/2}$ states. Inclusion of the Breit interaction, in addition to the Coulomb interaction, in the energy matrices for the intermediate-coupling calculations is found to have a pronounced effect on some multiplet Auger rates. The Breit interaction strongly influences the fine-structure splitting of some states, and, e.g., reverses the $^4P_{3/2}$-$^4P_{1/2}$ level order above $Z \simeq 75$.

## I. INTRODUCTION

The properties of multiply ionized atoms are important in connection with astrophysics and with the physics of atomic collisions and laser-induced plasmas. The spectra of the Li-like $1s2s2p$ configuration have been observed experimentally.[1-3] Several calculations have been performed for this configuration to predict x-ray transition energies and rates and Auger transition rates.[4-8] These calculations are nonrelativistic except for the work of Cheng, Lin, and Johnson[5] on the $^4P_{5/2}$ state.

In this paper we report on relativistic Hartree-Slater calculations of multiplet Auger and x-ray energies and transition rates, performed in the intermediate-coupling scheme for the $1s2s2p$ configuration of Li-like ions of 12 elements with atomic numbers $13 \leq Z \leq 92$.

## II. THEORY

### A. Multiplet Auger transition rates

The radiationless transition probability is calculated from perturbation theory assuming frozen orbitals.[9,10] The transition rate is given by the familiar "golden rule No. 2" as

$$T = \frac{2\pi}{\hbar} \left| \left\langle \psi_f \left| \sum_{i<j} V_{ij} \right| \psi_i \right\rangle \right|^2 \rho(\epsilon) \ . \tag{1}$$

Here, $\psi_i$ and $\psi_f$ are the antisymmetrized many-electron wave functions of the initial and final states of the ion, respectively, $\rho(\epsilon)$ is the energy density of final states, and $V_{ij}$ is the two-electron interaction operator.

In the present work, the two-electron operator $V_{ij}$ is chosen to be the original Møller operator, which is suitable for the local-potential approximation[10,11]:

$$V_{ij} = (1 - \vec{\alpha}_i \cdot \vec{\alpha}_j) \exp(i\omega r_{ij})/r_{ij} \ . \tag{2}$$

This form of the operator includes the retarded Coulomb and current-current interactions. The $\vec{\alpha}_i$ are Dirac matrices and $\omega$ is the wave number of the virtual photon.

For the Dirac-Hartree-Slater model used here, the orbital wave functions are assumed to satisfy a set of Dirac-Fock equations with a local exchange potential. These wave functions have the form

$$\psi_{n\kappa m}(r) = \frac{1}{r} \begin{pmatrix} G_{n\kappa}(r)\Omega_{\kappa m} \\ iF_{n\kappa}(r)\Omega_{-\kappa m} \end{pmatrix}, \tag{3}$$

where

$$\Omega_{\kappa m} = \sum_{\mu} C(\tfrac{1}{2} l j; \mu, m-\mu) Y_{l\mu}(\theta, \varphi) \chi_{1/2, m-\mu} \tag{4}$$

and

$$\Omega_{-\kappa m} = \sum_{\mu} C(\tfrac{1}{2} \bar{l} j; \mu, m-\mu) Y_{\bar{l}\mu}(\theta, \varphi) \chi_{1/2, m-\mu} \tag{5}$$

with

$$\kappa = (l-j)(2j+1) \ . \tag{6}$$

The Auger matrix elements between three-electron $j$-$j$ coupled initial states $|j_1, j_2 j_3(J_{23}); JM\rangle$ and final three-electron coupled states $|j_1^2(J_1'), \epsilon j_4; JM\rangle$ can be separated by Racah algebra into angular parts multiplied by radial integrals. We find

 

$$\left\langle j_1^2(J_1'),\epsilon j_4;J'M'\left|\sum_{i<j}V_{ij}\right|j_1,j_2j_3(J_{23});JM\right\rangle$$

$$=\sqrt{2}\,(2J_1'+1)^{1/2}(2J_{23}+1)^{1/2}W(j_1j_1Jj_4;J_1'J_{23})\delta_{JJ'}\delta_{MM'}A(j_2j_3J_{23}M_{23}\to j_1j_4J_{23}M_{23}), \quad (7)$$

where $W(j_1j_1Jj_4;J_1'J_{23})$ is the Racah coefficient[12] and $A(j_2j_3J_{23}M_{23}\to j_1j_4J_{23}M_{23})$ is the two-electron coupled Auger matrix element

$$A(j_2j_3J_{23}M_{23}\to j_1j_4J_{23}M_{23})=D'+D''-E'-E'', \quad (8)$$

$$D'=\left\langle j_1j_4J_{23}M_{23}\left|\frac{1}{r_{12}}e^{i\omega r_{12}}\right|j_2j_3J_{23}M_{23}\right\rangle, \quad (9)$$

$$D''=\left\langle j_1j_4J_{23}M_{23}\left|\frac{1}{r_{12}}e^{i\omega r_{12}}(\vec{\alpha}_1\cdot\vec{\alpha}_2)\right|j_2j_3J_{23}M_{23}\right\rangle, \quad (10)$$

with similar expressions for $E'$ and $E''$ obtained by exchanging $j_2$ and $j_3$ in $D'$ and $D''$.

The two-electron Auger matrix elements have been derived in our previous work.[10] Expressions for $D'$ and $D''$ are given in Eqs. (11) and (19), respectively, of Ref. 10 where details are given. The transition rate, in atomic units, is

$$T_{fi}(JM\to J'M')=\left|\left\langle j_1^2(J_1'),\epsilon j_4;J'M'\left|\sum_{i<j}V_{ij}\right|j_1,j_2j_3(J_{23}),JM\right\rangle\right|^2. \quad (11)$$

Here, the continuum wave function $\epsilon j_4$ is normalized to represent one ejected electron per unit time.

### B. Multiplet x-ray emission rate $j_1j_2j_3(J_{23});J\to j_1^2(J_1'),j_2;J'$

From first-order perturbation theory, the emission of a photon of energy $\hbar\omega$ and momentum $\hbar k$ into a solid angle element $d\Omega$, with polarization vector $\vec{\epsilon}$, by an atom going from an initial state $i$ to a final state $f$, is given by

$$T_{fi}=\frac{\alpha\omega}{2\pi}\left|\left\langle\psi_f\left|\sum_j\vec{\alpha}_j\cdot\vec{\epsilon}e^{i\vec{k}\cdot\vec{r}}\right|\psi_i\right\rangle\right|^2 d\Omega, \quad (12)$$

where

$$\hbar\omega=\hbar kc=E_i-E_f. \quad (13)$$

For the three-electron $j$-$j$-coupled states, we have

$$\psi_i=|\,j_1,j_2j_3(J_{23});JM\rangle,\quad \psi_f=|\,j_1^2(J_1'),j_2;J'M'\rangle. \quad (14)$$

We follow the procedure of earlier calculations for atoms with an inner-shell vacancy.[13-16] The plane-wave radiation field is expanded in terms of multipoles, and Racah algebra is used to separate the angular part from the radial integrals. After some algebra, the multiplet x-ray emission rate in $j$-$j$ coupling for the three-electron configuration is found to be

$$T_{fi}=\sum_L(|D_L\times T_L^{(e)}|^2+|D_L\times T_L^{(m)}|^2), \quad (15)$$

where

$$D_L=\sqrt{2}\,(-1)^{J+J'+J_1'+L}[J_{23},J_1',J',j_1]^{1/2}\begin{Bmatrix}j_1 & j_1 & J_1'\\ J & L & J'\\ J_{23} & j_3 & j_2\end{Bmatrix}, \quad (16)$$

$$T_L^{(e)}=[2\alpha\omega(2j_3+1)]^{1/2}(-1)^{j_3+1/2}\left(\frac{2L+1}{L(L+1)}\right)^{1/2}\begin{pmatrix}j_1 & L & j_3\\ 1/2 & 0 & -1/2\end{pmatrix}\prod(l_1Ll_3)R_L(e), \quad (17)$$

$$R_L(e)=\int\frac{dr}{kr}\Big[L(L+1)j_L(kr)(F_1G_3-F_3G_1)+(\kappa_1-\kappa_3)(F_1G_3+F_3G_1)\Big(j_L(kr)+\frac{kr}{(2L+1)}[Lj_{L-1}(kr)-(L+1)j_{L+1}(kr)]\Big)\Big], \quad (18)$$

$$T_L^{(m)}=[2\alpha\omega(2j_3+1)]^{1/2}(-1)^{j_3+1/2}\left(\frac{2L+1}{L(L+1)}\right)^{1/2}\begin{pmatrix} j_1 & L & j_3 \\ 1/2 & 0 & -1/2\end{pmatrix}\prod(l_1 L+1\ l_3)R_L(m)\,, \tag{19}$$

$$R_L(m)=(\kappa_1+\kappa_3)\int(G_1F_3+F_1G_3)j_L(kr)dr\,, \tag{20}$$

$$\prod(l_1Ll_3)=\begin{cases}1 & \text{if } l_1+L+l_3 \quad \text{even},\\ 0 & \text{otherwise}.\end{cases} \tag{21}$$

Here, $T_L^{(e)}$ and $T_L^{(m)}$ are just the relativistic x-ray matrix elements for atoms with an inner-shell vacancy only, and we have used the notation $[j_1,j_2,j_3,\ldots]^{1/2}=[(2j_1+1)(2j_2+1)(2j_3+1)\cdots]^{1/2}$.

### C. Relativistic intermediate coupling

We use the $j$-$j$ coupled states as basis states. The mixing of states with the same total angular momentum due to the residual Coulomb interaction is then included. For the $1s2s2p$ initial configuration considered in the present work the total-angular-momentum $J=\frac{1}{2}$ and $J=\frac{3}{2}$ states, respectively, contain the following three mixing states:

$$J=\tfrac{1}{2}\begin{cases}(1)\ 1s,2s2p_{1/2}(0);\tfrac{1}{2}\,,\\ (2)\ 1s,2s2p_{1/2}(1);\tfrac{1}{2}\,,\\ (3)\ 1s,2s2p_{3/2}(1);\tfrac{1}{2}\,,\end{cases} \tag{22}$$

and

$$J=\tfrac{3}{2}\begin{cases}(4)\ 1s,2s2p_{1/2}(1);\tfrac{3}{2}\,,\\ (5)\ 1s,2s2p_{3/2}(1);\tfrac{3}{2}\,,\\ (6)\ 1s,2s2p_{3/2}(2);\tfrac{3}{2}\,.\end{cases} \tag{23}$$

The energy matrices obtained through Racah algebra are contained in Tables I and II. In these matrices $E$ and $E^1$ are the average energies of the configurations $1s2s2p_{1/2}$ and $1s2s2p_{3/2}$, respectively.

The eigenfunctions and eigenvalues are found by diagonalizing the energy matrices. The eigenstates for $J=\frac{1}{2}$ and $J=\frac{3}{2}$, with energies in descending order, are designated as $^2P_{1/2}^{(+)}$, $^2P_{1/2}^{(-)}$, $^4P_{1/2}$ and $^2P_{3/2}^{(+)}$, $^2P_{3/2}^{(-)}$, $^4P_{3/2}$, respectively. These eigenfunctions and eigenvalues are then used to calculate the Auger and x-ray energies in intermediate coupling. The reader is referred to our previous work on $K$-$LL$ Auger spectra for details.[17]

In order to investigate the effect of the Breit interaction[18] on the fine structure and multiplet transition rates, we have repeated the intermediate-coupling calculations with not only the Coulomb interaction but also the Breit interaction in the energy matrices. For the three-electron configuration the Coulomb- and Breit-interaction matrix is

TABLE I. Energy matrix for the mixing calculation of $J=\frac{1}{2}$ states listed in Eq. (22).

| | (1) | (2) | (3) |
|---|---|---|---|
| (1) | $E-\frac{1}{6}G^1(2s2p_{1/2})$ | $-\frac{\sqrt{3}}{2}G^0(1s2s)$ | $-\frac{1}{3}(\frac{2}{3})^{1/2}\ R_1(1s2p_{1/2}2p_{3/2}1s)$ |
| | | $-\frac{1}{6\sqrt{3}}G^1(1s2p_{1/2})$ | |
| (2) | $-\frac{\sqrt{3}}{2}G^0(1s2s)$ | $E+\frac{1}{18}G^1(2s2p_{1/2})$ | $-\frac{2\sqrt{2}}{9}R^1(1s2p_{1/2}2p_{3/2}2s)$ |
| | $-\frac{1}{6\sqrt{3}}G^1(1s2p_{1/2})$ | $+G^0(1s2s)-\frac{1}{9}G^1(1s2p_{1/2})$ | $+\frac{\sqrt{2}}{9}R^1(1s2p_{1/2}2p_{3/2}1s)$ |
| (3) | $-\frac{1}{3}(\frac{2}{3})^{1/2}\ R^1(1s2p_{1/2}2p_{3/2}1s)$ | $-\frac{2\sqrt{2}}{9}R^1(2s2p_{1/2}2p_{3/2}2s)$ | $E^1+\frac{5}{18}G^1(2s2p_{3/2})$ |
| | | $+\frac{\sqrt{2}}{9}R^1(1s2p_{1/2}2p_{3/2}1s)$ | $-\frac{1}{2}G^0(1s2s)+\frac{5}{18}G^1(1s2p_{3/2})$ |

TABLE II. Energy matrix for the mixing calculation of $J=\frac{3}{2}$ states listed in Eq. (23).

| | (4) | (5) | (6) |
|---|---|---|---|
| (4) | $E+\frac{1}{18}G^1(2s2p_{1/2})$<br>$-\frac{1}{2}G^0(1s2s)+\frac{1}{18}G^1(1s2p_{1/2})$ | $-\frac{2\sqrt{2}}{9}R^1(2s2p_{1/2}2p_{3/2}2s)$<br>$-\frac{\sqrt{2}}{18}R^1(1s2p_{1/2}2p_{3/2}1s)$ | $-\frac{1}{3}(\frac{5}{6})^{1/2}\ R^1(1s2p_{1/2}2p_{3/2}1s)$ |
| (5) | $-\frac{2\sqrt{2}}{9}R^1(2s2p_{1/2}2p_{3/2}2s)$<br>$-\frac{\sqrt{2}}{18}R^1(1s2p_{1/2}2p_{3/2}1s)$ | $E^1+\frac{5}{18}G^1(2s2p_{3/2})$<br>$+\frac{1}{4}G^0(1s2s)-\frac{5}{36}G^1(1s2p_{3/2})$ | $-\frac{\sqrt{15}}{4}G^0(1s2s)$<br>$+\frac{1}{12}(\frac{5}{3})^{1/2}\ G^1(1s2p_{3/2})$ |
| (6) | $-\frac{1}{3}(\frac{5}{6})^{1/2}\ R^1(1s2p_{1/2}2p_{3/2}1s)$ | $-\frac{\sqrt{15}}{4}G^0(1s2s)$<br>$+\frac{1}{12}(\frac{5}{3})^{1/2}\ G^1(1s2p_{3/2})$ | $E^1-\frac{1}{6}G^1(2s2p_{3/2})$<br>$+\frac{3}{4}G^0(1s2s)+\frac{1}{4}G^1(1s2p_{3/2})$ |

$$\left\langle j_1, j_2 j_3(J_{23}); JM \left| \sum_{i<j} V_{ij}^{(R)} \right| j_1', j_2' j_3'(J_{23}'); JM \right\rangle$$

$$= \delta_{J_{23}J_{23}'}\delta_{j_1j_1'}(j_2 j_3 J_{23}M_{23}|\, V_{23}^{(R)}\,|j_2' j_3' J_{23}M_{23})$$

$$+\sum_{J_{12}} [J_{12}, J_{12}, J_{23}, J_{23}']^{1/2} W(j_1 j_2 J j_3; J_{12} J_{23}) W(j_1' j_2' J j_3'; J_{12} J_{23}') \delta_{j_3 j_3'}(j_1 j_2 J_{12}M_{12}|\, V_{12}^{(R)}\,|j_1' j_2' J_{12}M_{12})$$

$$+\sum_{J_{13}} [J_{13}, J_{13}, J_{23}, J_{23}', ]^{1/2} W(j_1 j_3 J j_2; J_{13} J_{23}) W(j_1' j_3' J j_2'; J_{13} J_{23}') \delta_{j_2 j_2'}(j_1 j_3 J_{13}M_{13}|\, V_{13}^{(R)}\,|j_1' j_3' J_{13}M_{13})$$

$$\times(-1)^{j_2+j_3-J_{23}+j_2'+j_3'-J_{23}'}. \tag{24}$$

Here, $V_{ij}^{(R)}$ is the real part of $V_{ij}$ as given in Eq. (2), $W(abcd;ef)$ is the Wigner $W$ coefficient, and $(j_1 j_2 J_{12}M_{12}|\, V_{12}^{(R)}\,|j_1' j_2' J_{12}M_{12})$ is the two-electron coupled Coulomb- and Breit-interaction matrix element, which is just the real part of the general relativistic Auger matrix element derived in Ref. 10.

## III. NUMERICAL CALCULATIONS

The relativistic Auger and x-ray matrix elements in $j$-$j$ coupling were calculated from Dirac-Hartree-Slater (DHS) wave functions that correspond to the appropriate initial electron configurations. The average transition energies used in

TABLE III. Calculated $K$ x-ray energies (in eV) for the $1s2s2p$ configuration of Li-like ions.

| Initial state | Atomic number 13 | 18 | 20 | 22 | 25 | 26 | 30 |
|---|---|---|---|---|---|---|---|
| $^2P_{1/2}^{(+)}$ | 1588.24 | 3125.09 | 3885.66 | 4730.43 | 6157.88 | 6676.35 | 8969.91 |
| $^2P_{3/2}^{(+)}$ | 1588.35 | 3125.71 | 3886.66 | 4731.93 | 6160.29 | 6679.24 | 8974.67 |
| $^2P_{1/2}^{(-)}$ | 1579.28 | 3112.29 | 3870.88 | 4713.22 | 6136.07 | 6652.01 | 8933.54 |
| $^2P_{3/2}^{(-)}$ | 1579.70 | 3114.01 | 3873.64 | 4717.49 | 6143.44 | 6661.43 | 8952.61 |
| $^4P_{1/2}$ | 1561.77 | 3086.34 | 3841.40 | 4680.09 | 6097.39 | 6611.34 | 8885.14 |
| $^4P_{3/2}$ | 1561.95 | 3087.20 | 3842.74 | 4682.07 | 6100.47 | 6615.07 | 8891.13 |
| $^4P_{5/2}$ | 1562.43 | 3089.31 | 3846.14 | 4687.31 | 6109.46 | 6626.44 | 8913.47 |

TABLE IV. Calculated $K$-shell Auger energies (in eV) for the $1s2s2p$ configuration of Li-like ions.

| Initial state | Atomic number 13 | 18 | 20 | 22 | 25 | 26 | 30 |
|---|---|---|---|---|---|---|---|
| $^2P_{1/2}^{(+)}$ | 1146.12 | 2207.19 | 2728.82 | 3304.58 | 4276.98 | 4630.64 | 6186.32 |
| $^2P_{3/2}^{(+)}$ | 1146.24 | 2207.81 | 2729.82 | 3306.09 | 4279.39 | 4633.54 | 6191.08 |
| $^2P_{1/2}^{(-)}$ | 1137.17 | 2194.38 | 2714.05 | 3287.38 | 4255.17 | 4606.30 | 6149.95 |
| $^2P_{3/2}^{(-)}$ | 1137.58 | 2196.10 | 2716.81 | 3291.64 | 4262.54 | 4615.73 | 6169.01 |
| $^4P_{1/2}$ | 1119.65 | 2168.44 | 2684.56 | 3254.24 | 4216.49 | 4565.63 | 6101.54 |
| $^4P_{3/2}$ | 1119.84 | 2169.29 | 2685.90 | 3256.22 | 4219.58 | 4569.36 | 6107.54 |
| $^4P_{5/2}$ | 1120.33 | 2171.40 | 2689.30 | 3261.47 | 4228.57 | 4580.73 | 6129.88 |

the present calculations were found by performing separate self-consistent-field calculations for the initial and final configurations, thus automatically including relaxation energies. Contributions due to quantum-electrodynamic corrections, such as Breit interaction, vacuum polarization, and $K$-shell self-energy, were also included in the energy calculations.[19] The electrostatic Slater integrals required for the intermediate-coupling calculations were computed with DHS wave functions. The two-electron coupled Coulomb- and Breit-interaction matrix elements were calculated with the slightly modified general Auger program.[10,20] We use the configuration average energies for calculating the x-ray and Auger matrix elements.

TABLE V. Comparison between theoretical and experimental x-ray energies for $1s2s2p \rightarrow 1s^22s$ transitions. (All energies in eV.)

| Atomic number | Initial state | Energy Present theory | Experiment[a,b] |
|---|---|---|---|
| 13 | $^2P^{(-)}$ | 1579.6 | 1579.6 |
| 18 | $^2P_{1/2}^{(-)}$ | 3112.3 | 3111.4 |
| | $^2P_{3/2}^{(-)}$ | 3114.0 | 3113.3 |
| | $^4P_{3/2}$ | 3087.2 | 3087.5 |
| | $^4P_{5/2}$ | 3089.3 | 3089.7 |
| 22 | $^4P$ | 4682.9 | 4682.2 |
| | $^2P^{(-)}$ | 4716.1 | 4715.1 |
| 26 | $^2P_{1/2}^{(-)}$ | 6652.0 | 6655.5 |
| | $^2P_{3/2}^{(-)}$ | 6661.4 | 6662.3 |
| | $^2P_{1/2}^{(+)}$ | 6676.4 | 6676.6 |

[a] References 1 and 21.

[b] C. Corliss and J. Sugar, J. Phys. Chem. Ref. Data 4, 353 (1975); 8, 1 (1979).

## IV. RESULTS AND DISCUSSION

The x-ray and Auger transition energies for seven elements with atomic numbers $13 \leq Z \leq 30$ are listed in Tables III and IV. Contributions to the transition energies from electron-electron Coulomb correlation (~1 eV) are not included. The x-ray energies found in the present work agree quite well with Vainshtein and Safronova's calculations using charge-expansion perturbation

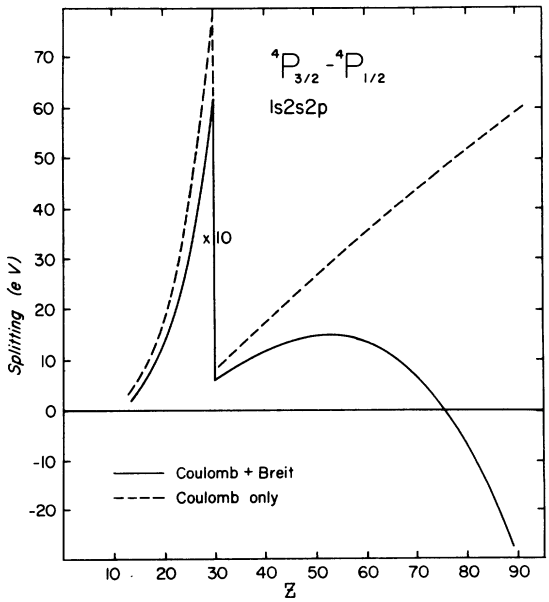


FIG. 1. Fine-structure splitting (in eV) between $^4P_{3/2}$ and $^4P_{1/2}$ levels of Li-like ions with the $1s2s2p$ configuration as a function of atomic number. When the Breit interaction is included in the energy matrix that determines the intermediate-coupling coefficients ("Coulomb + Breit"), the splitting is reduced and the level order is actually reversed above $Z \cong 75$.

TABLE VI. Theoretical Auger and x-ray emission rates (in atomic units) for the $^2P^{(+)}_{1/2}$, $^2P^{(-)}_{1/2}$, and $^2P^{(+)}_{3/2}$ states of the $1s2s2p$ configuration of Li-like ions.[a]

| | $^2P^{(+)}_{1/2}$ | | | $^2P^{(-)}_{1/2}$ | | | $^2P^{(+)}_{3/2}$ | | |
|---|---|---|---|---|---|---|---|---|---|
| $Z$ | Auger | X ray | Total | Auger | X ray | Total | Auger | X ray | Total |
| 13 | 2.13(−3) | 8.49(−5) | 2.21(−3) | 2.28(−4) | 5.83(−4) | 8.11(−4) | 2.18(−3) | 5.56(−5) | 2.24(−3) |
| 18 | 2.21(−3) | 4.67(−4) | 2.68(−3) | 4.05(−4) | 2.17(−3) | 2.58(−3) | 2.42(−3) | 1.33(−4) | 2.55(−3) |
| 20 | 2.18(−3) | 8.63(−4) | 3.04(−3) | 5.27(−4) | 3.23(−3) | 3.76(−3) | 2.50(−3) | 1.47(−4) | 2.65(−3) |
| 22 | 2.11(−3) | 1.53(−3) | 3.64(−3) | 6.86(−4) | 4.54(−3) | 5.23(−3) | 2.56(−3) | 1.37(−4) | 2.70(−3) |
| 25 | 1.98(−3) | 3.21(−3) | 5.19(−3) | 9.58(−4) | 7.01(−3) | 7.97(−3) | 2.64(−3) | 8.41(−5) | 2.72(−3) |
| 26 | 1.88(−3) | 4.25(−3) | 6.13(−3) | 1.10(−3) | 7.80(−3) | 8.90(−3) | 2.66(−3) | 4.56(−5) | 2.71(−3) |
| 30 | 1.59(−3) | 9.74(−3) | 1.133(−2) | 1.60(−3) | 1.175(−2) | 1.335(−2) | 2.72(−3) | 1.77(−5) | 2.74(−3) |
| 36 | 1.21(−3) | 2.514(−2) | 2.635(−2) | 2.36(−3) | 1.928(−2) | 2.164(−2) | 2.76(−3) | 8.97(−4) | 3.66(−3) |
| 54 | 6.05(−4) | 1.499(−1) | 1.505(−1) | 4.84(−3) | 6.517(−2) | 7.001(−2) | 3.00(−3) | 2.229(−2) | 2.529(−2) |
| 67 | 3.94(−4) | 3.568(−1) | 3.572(−1) | 7.60(−3) | 1.338(−1) | 1.414(−1) | 3.38(−3) | 7.128(−2) | 7.466(−2) |
| 80 | 2.73(−4) | 7.116(−1) | 7.119(−1) | 1.209(−2) | 2.435(−1) | 2.556(−1) | 3.91(−3) | 1.688(−1) | 1.728(−1) |
| 92 | 2.35(−4) | 1.204 | 1.204 | 1.912(−2) | 3.876(−1) | 4.067(−1) | 4.54(−3) | 3.194(−1) | 3.244(−1) |

[a] Numbers in parentheses stand for powers of ten, e.g., $2.12(-3) = 2.12\times10^{-3}$.

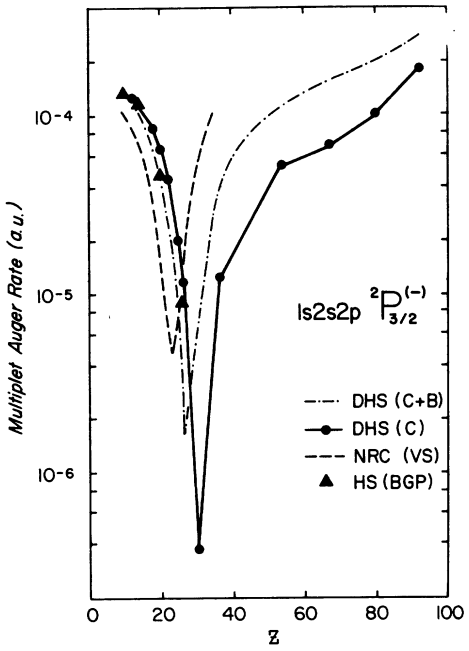


FIG. 2. Relativistic multiplet Auger decay rates of the $1s2s2p\ ^2P^{(-)}_{3/2}$ state calculated in intermediate coupling as a function of atomic number. The curve labeled DHS (C + B) was computed including both Breit and Coulomb interactions in the energy matrices that determine the intermediate-coupling coefficients; the curve labeled DHS(C) was computed including only the Coulomb interaction in these matrices. For comparison, two sets of nonrelativistic intermediate-coupling results are shown: those of Vainshtein and Safronova based on Coulomb wave functions (Ref. 6) labeled NRC (VS), and those of Bhalla *et al.* based on Hartree-Slater wave functions (Ref. 4) labeled HS (BGP). All rates are given in atomic units (1 a.u. $= 4.134\times10^{16}$ sec$^{-1}$).

theory[6]: the discrepancies range from ~1 eV at $Z=20$ to ~4 eV at $Z=30$. Our x-ray energies also agree well with experiment (Table V). The present theoretical DHS results for the Auger and x-ray emission rates in intermediate coupling (including the Breit interaction) are listed in Tables VI and VII.

The effect of the Breit interaction on fine-structure splitting is quite important for some of the states, especially for the splitting between $^4P_{3/2}$ and $^4P_{1/2}$. The Breit interaction reduces the $^4P_{3/2}$-$^4P_{1/2}$ splitting and reverses the order of these two levels above $Z\cong75$ (Fig. 1). For two elements, $^4P$ splitting has been calculated both by Cheng, Desclaux, and Kim[5] with a Dirac-Fock (DF) code and by us in the DHS model. Agreement is excellent: for the $1s2s2p\ ^4P^o$ $\frac{5}{2}$-$\frac{3}{2}$ splitting, the DF results are 3.39 eV and 11.35 eV for $Z=20$ and $Z=26$, respectively, while our DHS results are 3.40 eV and 11.37 eV. For the $J=\frac{3}{2}$-$\frac{1}{2}$ splitting, the DF results are 1.33 eV and 3.70 eV for $Z=20$ and $Z=26$, respectively, while the DHS results are 1.34 eV and 3.73 eV.

In Figs. 2–5 our calculated DHS multiplet Auger rates in intermediate coupling are compared with nonrelativistic intermediate-coupling calculations.[4] For states with large Auger decay rates (e.g., $^2P^{(+)}$), the differences between our relativistic DHS results and nonrelativistic Hartree-Slater (HS) values are ~10%, while for $^4P_{1/2,3/2}$ states they differ by as much as two orders of magnitude. The results from calculations using Coulomb wave functions[6] are quite different from those based on self-consistent-

TABLE VII. Theoretical Auger and x-ray emission rates (in atomic units) for the $^2P_{3/2}^{-}$, $^4P_{1/2}$, $^4P_{3/2}$, and $^4P_{5/2}$ states of the $1s2s2p$ configuration of Li-like ions.[a]

| | $^2P_{3/2}^{-}$ | | | $^4P_{1/2}$ | | | $^4P_{3/2}$ | | | $^4P_{5/2}$ | |
|---|---|---|---|---|---|---|---|---|---|---|---|
| $Z$ | Auger | X ray | Total | Auger | X ray | Total | Auger | X ray | Total | Auger | X ray | Total |
| 13 | 1.17(−4) | 6.12(−4) | 7.29(−4) | 1.02(−7) | 1.53(−7) | 2.55(−7) | 2.85(−9) | 3.95(−7) | 3.98(−7) | 8.08(−9) | 5.07(−10) | 8.59(−9) |
| 18 | 6.74(−5) | 2.50(−3) | 2.57(−3) | 2.41(−7) | 4.03(−6) | 4.27(−6) | 2.71(−7) | 1.11(−5) | 1.14(−5) | 3.32(−8) | 7.65(−9) | 4.09(−8) |
| 20 | 4.48(−5) | 3.39(−3) | 3.97(−3) | 3.22(−7) | 1.11(−5) | 1.14(−5) | 7.21(−7) | 3.16(−5) | 3.23(−5) | 5.21(−8) | 1.83(−8) | 7.04(−8) |
| 22 | 2.51(−5) | 5.88(−3) | 5.91(−3) | 4.42(−7) | 2.74(−5) | 2.78(−5) | 1.60(−6) | 8.08(−5) | 8.24(−5) | 7.81(−8) | 4.02(−8) | 1.18(−7) |
| 25 | 6.19(−6) | 9.96(−3) | 9.97(−3) | 8.41(−7) | 8.45(−5) | 8.53(−5) | 3.71(−6) | 2.61(−4) | 2.65(−4) | 1.34(−7) | 1.14(−7) | 2.48(−7) |
| 26 | 1.72(−6) | 1.173(−2) | 1.173(−2) | 9.26(−7) | 1.25(−4) | 1.26(−4) | 5.63(−6) | 3.99(−4) | 4.05(−4) | 1.58(−7) | 1.59(−7) | 3.17(−7) |
| 30 | 5.61(−6) | 2.046(−2) | 2.047(−2) | 2.25(−6) | 4.25(−4) | 4.27(−4) | 1.40(−5) | 1.43(−3) | 1.44(−3) | 2.87(−7) | 5.13(−7) | 8.00(−7) |
| 36 | 3.97(−5) | 3.921(−2) | 3.925(−2) | 8.96(−6) | 1.74(−3) | 1.75(−3) | 3.27(−5) | 6.05(−3) | 6.08(−3) | 6.12(−7) | 2.28(−6) | 2.89(−6) |
| 54 | 1.18(−4) | 1.493(−1) | 1.494(−1) | 1.88(−4) | 2.303(−2) | 2.322(−2) | 4.24(−5) | 6.654(−2) | 6.658(−2) | 3.21(−6) | 6.27(−5) | 6.59(−5) |
| 67 | 1.55(−4) | 3.104(−1) | 3.106(−1) | 7.80(−4) | 7.328(−2) | 7.406(−2) | 1.76(−5) | 1.826(−1) | 1.826(−1) | 7.61(−6) | 3.68(−4) | 3.76(−4) |
| 80 | 2.03(−4) | 5.709(−1) | 5.711(−1) | 2.41(−3) | 1.806(−1) | 1.830(−1) | 8.67(−5) | 3.974(−1) | 3.975(−1) | 1.51(−5) | 1.59(−3) | 1.61(−3) |
| 92 | 2.71(−4) | 9.173(−1) | 9.176(−1) | 6.00(−3) | 3.615(−1) | 3.675(−1) | 4.07(−4) | 7.213(−1) | 7.217(−1) | 2.49(−5) | 5.09(−3) | 5.11(−3) |

[a] Numbers in parentheses stand for powers of ten, e.g., $1.30(-4) = 1.30 \times 10^{-4}$.

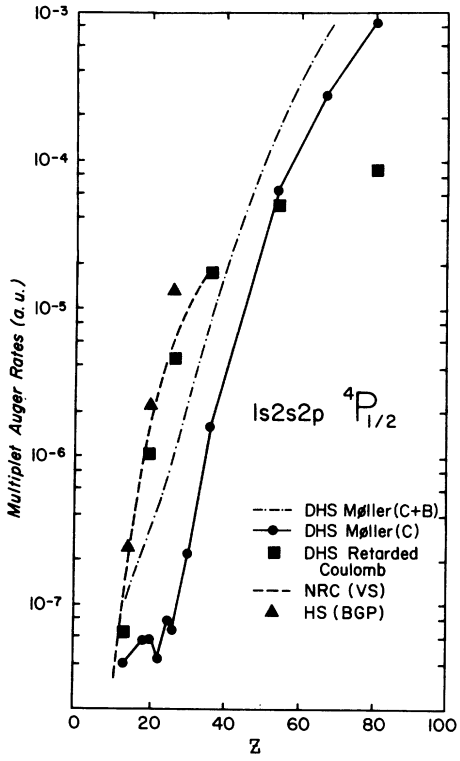


FIG. 3. Relativistic multiplet Auger decay rates of the $1s2s2p\ ^4P_{1/2}$ state computed in intermediate coupling: the results labeled DHS Møller (C + B) were obtained with the full Møller operator and included both Coulomb and Breit interactions in the energy matrices that determine the intermediate-coupling coefficients; the curve labeled DHS Møller (C) was computed with the full Møller operator but included only the Coulomb interaction in the energy matrices for the intermediate-coupling calculations. The rates labeled DHS Retarded Coulomb were calculated with the retarded Coulomb interaction alone instead of the full Møller operator. For comparison, nonrelativistic results are shown: The rates labeled NRC (VS) were calculated from Coulomb wave functions (Ref. 6); the rates labeled HS (BGP) were calculated from Hartree-Slater wave functions (Ref. 4). Rates are indicated in atomic units (1 a.u. $= 4.134 \times 10^{16}$ sec$^{-1}$) as functions of atomic number $Z$.

field models.

The weak transitions usually involve large cancellations. Consequently, such transitions are very sensitive to differences in atomic models. This is illustrated by comparing Auger rates computed with the full Møller operator with rates computed with the retarded Coulomb interaction alone (Figs. 3 and 4). It is seen that inclusion of the retarded current-current interaction through the Møller operator can change the transition rates for $^4P_{1/2}$ and $^4P_{3/2}$ states by as much as one full order of magnitude. The importance of relativistic effects in the transition rates from

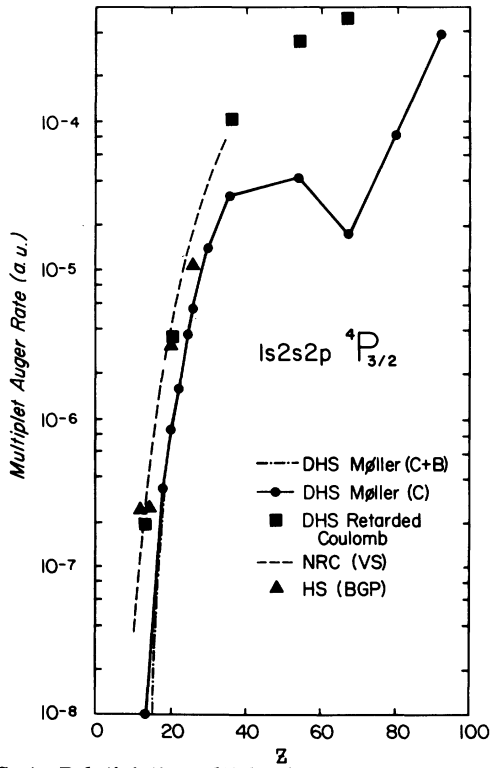


FIG. 4. Relativistic multiplet Auger decay rates of the $1s2s2p\ ^2P_{3/2}$ state calculated in intermediate coupling: The results labeled DHS Møller (C + B) were obtained with the full Møller operator and included both Coulomb and Breit interactions in the energy matrices that determine the intermediate-coupling coefficients; the curve labeled DHS Møller (C) was computed with the full Møller operator but included only the Coulomb interaction in the energy matrices for the intermediate-coupling calculations. For comparison, nonrelativistic results derived with Coulomb wave functions [Ref. 6; NRC (VS)] and with Hartree-Slater wave functions [Ref. 4; HS (BGP)] are shown. Rates are given in atomic units as functions of atomic number $Z$.

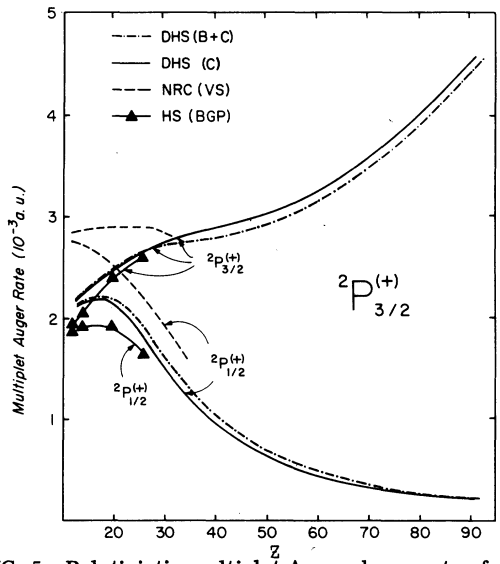


FIG. 5. Relativistic multiplet Auger decay rates for the $1s2s2p\ ^2P^{(+)}_{1/2,3/2}$ states calculated in intermediate coupling: the results labeled DHS (B+C) were obtained by including both the Breit and Coulomb interactions in the energy matrices that determine the intermediate-coupling coefficients; the curve labeled DHS (C) was computed including only the Coulomb interaction in the energy matrices for the intermediate-coupling calculations. For comparison, nonrelativistic results derived with Coulomb wave functions [Ref. 6; NRC (VS)] and with Hartree-Slater wave functions [Ref. 4; HS (BGP)] are shown. Rates are given in milliatomic units (1 ma.u. = $4.134\times10^{13}$ sec$^{-1}$) as functions of atomic number $Z$.

$^4P$ states for relatively small atomic numbers is clearly seen in Figs. 3 and 4.

Inclusion of the Breit interaction in the intermediate-coupling calculation has an important effect on states with small transition rates, such as $^2P^{(-)}_{3/2}$ and $^4P_{1/2}$ (Figs. 2, 3), but affects states with large transition rates (e.g., $^2P^{(+)}$) by only a few percent (Fig. 5).

The $^4P_{5/2}$ state decays via a radiative magnetic-quadrupole ($M2$) transition in the x-ray branch and through spin-spin interaction in the Auger branch.[5] The lifetime of the $^4P_{5/2}$ state from the present DHS calculations is compared with results from previous DHS calculations[5] and with experiment[21,22] in Fig. 6. Discrepancies between the present Auger rates and those from previous DHS

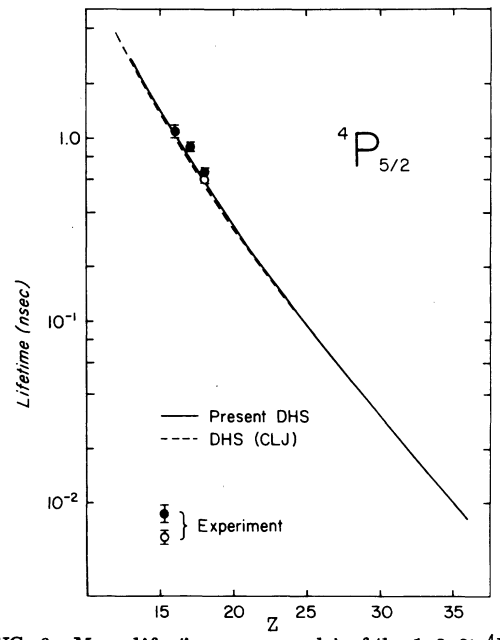


FIG. 6. Mean life (in nanoseconds) of the $1s2s2p\ ^4P_{5/2}$ state as a function of atomic number $Z$. Result from the present relativistic DHS calculations are compared with the DHS results of Cheng, Lin, and Johnson (Ref. 5) labeled DHS (CLJ) and with experimental values (Refs. 21 and 22).

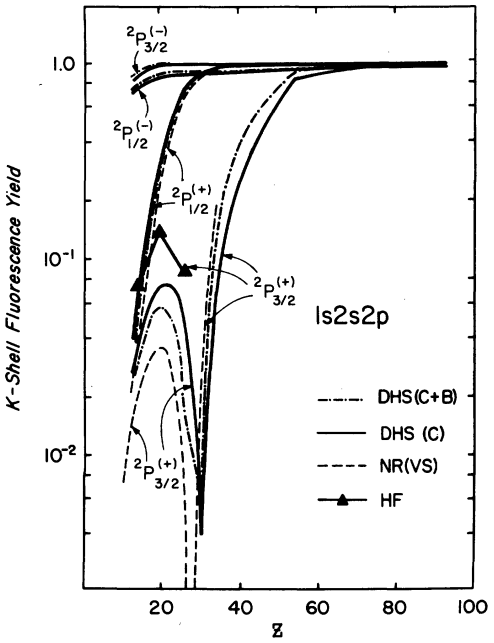


FIG. 7. $K$-shell fluorescence yields of the $^2P$ multiplet states of the $1s2s2p$ configuration as functions of atomic number $Z$. Results from the present relativistic calculations are shown: the fluorescence yields labeled DHS (C + B) were computed including both the Coulomb and Breit interactions in the energy matrices that determine the intermediate-coupling coefficients, while for the results labeled DHS (C) only the Coulomb interaction was included in these matrices. For comparison, nonrelativistic results are also shown: NR (VS) computed with hydrogenic wave functions (Ref. 6), and HF computed with Hartree-Fock wave functions (Ref. 7).

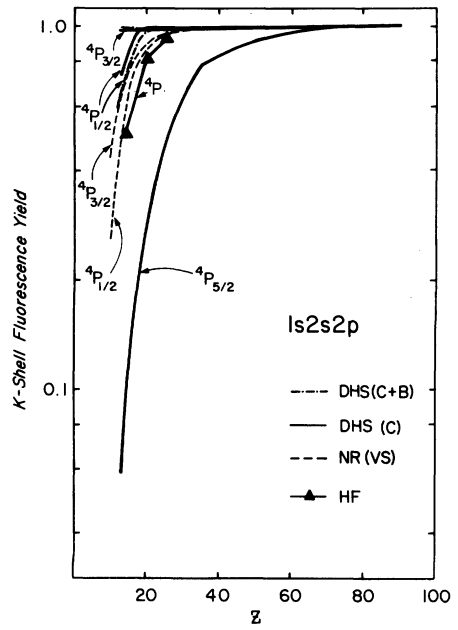


FIG. 8. $K$-shell fluroescence yields of the $^4P$ multiplet states of the $1s2s2p$ configuration as functions of atomic number $Z$. Results from the present relativistic calculations are shown: the fluorescence yields labeled DHS (C + B) were computed including both the Coulomb and Breit interactions in the energy matrices that determine the intermediate-coupling coefficients, while for the results labeled DHS (C) only the Coulomb interaction was included in these matrices. The DHS yields are compared with those from nonrelativistic hydrogenic calculations [Ref. 6, NR (VS)] and Hartree-Fock calculations [Ref. 7, HF].

calculations[5] range from ~10% at $Z=13$ to ~3% at $Z=26$. These differences could be due to the fact that we include the transverse correction[18] in our calculations. For the x-ray decay rate of the $^4P_{5/2}$ state, results from our present DHS calculations agree with those from early DHS calculations[5] to better than 2% for all atomic numbers. Our present theoretical lifetimes of $^4P_{5/2}$ states agree within experimental uncertainty with measured data for Ar that have been corrected for cascade contributions.[21]

The $K$-shell fluorescence yields for multiplet states of the $1s2s2p$ configuration are shown in Figs. 7 and 8 as functions of atomic number; we compare results from the present DHS intermediate-coupling calculations with those from nonrelativistic Hartree-Fock[7] and hydrogenic[6] calculations. The multiplet fluorescence yields are seen to be quite sensitive to the atomic model. The present DHS intermediate-coupling calculations predict much higher fluorescence yields for low-$Z$ $^4P_{1/2}$ and $^4P_{3/2}$ states than predicted by nonrelativistic calculations.[6,7] For the $^2P^{(+)}_{3/2}$ state there is a strong accidental cancellation in the radiative matrix element near $Z=30$. Consequently, the fluorescence yield of this state in the vicinity of $Z=30$ is exceptionally sensitive to relativistic effects and to the details of the atomic model.

Accurate experimental determinations of the $^4P$-state lifetimes and the average fluorescence yield of the $1s2s2p$ configuration would be most useful.

This work was supported in part by the Air Force Office of Scientific Research (Grant No. 79-0026).

*Present address: Code AD, National Aeronautics and Space Administration, Washington, D.C. 20546.
[1]V. A. Boiko, A. Ya Faenov, and S. A. Pikuz, J. Quant. Spectrosc. Radiat. Transfer 19, 11 (1978).
[2]E. Ya Gol'ts, U. I. Zitnik, E. Ya Kononov, S. L. Mandel'shtam, and Yu V. Sidel'nikov, Dokl. Akad. Nauk SSSR 220, 560 (1975) [Sov. Phys.—Dokl. 20, 49 (1975)].
[3]E. V. Aglitsky, V. A. Boiko, S. M. Zaharov, S. A. Pikuz, and A. Yu Faenov, Kuant. Electron. (Moscow) 1, 908 (1974) [Sov. J. Quantum Electron 4, 500 (1974)].
[4]C. P. Bhalla, A. H. Gabriel, and L. P. Presnyakov, Mon. Not. R. Astron. Soc. 172, 359 (1975).
[5]K. T. Cheng, C. P. Lin, and W. R. Johnson, Phys. Lett. 48A, 437 (1974); and private communication. See also K. T. Cheng, J. P. Desclaux, and Y.-K. Kim, J. Phys. B 11, L359 (1978).
[6]L. A. Vainshtein and U. I. Safronova, At. Data Nucl. Data Tables 21, 50 (1978).
[7]A. H. Gabriel, Mon. Not. R. Astron. Soc. 160, 99 (1972).
[8]M. H. Chen and B. Crasemann, Phys. Rev. A 12, 959 (1975).
[9]W. Bambynek, B. Crasemann, R. W. Fink, H. U. Freund, H. Mark, C. D. Swift, R. E. Price, and P. V. Rao, Rev. Mod. Phys. 44, 716 (1972).
[10]M. H. Chen, E. Laiman, B. Crasemann, and Hans Mark, Phys. Rev. 19, 2253 (1979).
[11]K. N. Huang, J. Phys. B 11, 787 (1978).
[12]M. E. Rose, *Elementary Theory of Angular Momentum* (Wiley, New York, 1957), Chap. VI.
[13]J. H. Scofield, in *Atomic Inner-Shell Processes*, edited by B. Crasemann (Academic, New York, 1975), Vol. I, p. 265.
[14]J. H. Scofield, Phys. Rev. 179, 9 (1969).
[15]H. R. Rosner and C. P. Bhalla, Z. Phys. 231, 347 (1970).
[16]I. P. Grant, J. Phys. B 7, 1458 (1974).
[17]M. H. Chen, B. Crasemann, and H. Mark, Phys. Rev. A 21, 442 (1980).
[18]J. B. Mann and W. R. Johnson, Phys. Rev. A 4, 41 (1971).
[19]K.-N. Huang, M. Aoyagi, M. H. Chen, B. Crasemann, and H. Mark, At. Data Nucl. Data Tables 18, 243 (1976).
[20]M. H. Chen (unpublished).
[21]H. D. Dohmann and R. Mann, Z. Phys. A 291, 15 (1979).
[22]D. J. Pegg, H. H. Haselton, P. M. Griffin, R. Laubert, J. R. Mowat, R. Peterson, and I. A. Sellin, Phys. Rev. A 9, 1112 (1974).